Supplemental Materials

Molecular Biology of the Cell

Stout and Spray

Cysteine residues in the cytoplasmic carboxyl terminus of connexins dictate gap junction plaque stability.

Randy F. Stout, Jr.[*†‡], David C. Spray[†]

[*]Department of Biomedical Sciences

New York Institute of Technology College of Osteopathic Medicine

Old Westbury, NY 11568-0000, USA

[†]Dominick P. Purpura Department of Neuroscience

Albert Einstein College of Medicine,

1410 Pelham Parkway South, Bronx, NY 10461, USA

[‡]Corresponding author: rstout@nyit.edu

Running Head: Determinants of gap junction plaque organization

Abbreviations: Cx, connexin; Cx26, connexin 26; Cx26CT43, rat Cx26 with a 30 amino acid sequence from the CT of Connexin 43 appended to the carboxyl-terminus of Cx26; Cx30, connexin 30; Cx32, Connexin 32, Cx43, connexin 43; EBFP2, enhanced blue fluorescent protein 2; FRAP, fluorescence recovery after photobleaching; GFP, green fluorescent protein; HEPES, (4-(2-hydroxyethyl)-1-piperazineethanesulfonic acid; msfGFP, monomerized superfolder green fluorescent protein; ROI, region of interest; RT, room temperature; sfGFP, non-monomerized superfolder green fluorescent protein; Cx43d20AA, rat Cx43 with 20 amino acids residues 241-260 resected; GFP-Cx43t*XXX,* rat Cx43 tagged with GFP on the amino-terminus truncated at the indicated amino acid (i.e. GFP-Cx43t258 is truncated by mutagenesis of lysine 258 to a stop codon); Cx43cyslCT, rat Cx43 with cysteine residues 260, 271, and 298 mutated to alanine; Cx32cyslCT, human Cx32 with cysteine residues 280 and 283 mutated to alanine.

SUPPLEMENTAL MATERIALS

Plasmids and Subcloning:

Plasmids used in the publication and not described previously elsewhere will be made available from the online plasmid consortium Addgene.org. Cx43-msfGFP, Cx30-msfGFP, Cx26-msfGFP, msfGFP-Cx43, Cx43K258stop-msfGFP, sfGFP-Cx26, sfGFP-Cx43K258stop were described previously (Stout, Snapp et al. 2015). pLv-eEF1α-Cx43_CMV-mCherry and pLv-eEF1α-Cx43cyslCT_CMV-mCherry were produced by the plasmid construction service of VectorBuilder

Inc. sfGFP-Cx43cyslCT and msfGFP-Cx32cyslCT were produced by mutagenesis and/or gene synthesis by the plasmid construction service of Genscript Inc. sfGP-Cx43m262, sfGFP-Cx43m268, and sfGFP-Cx43m273 were produced by using PCR amplification and subcloning with primers designed to insert a stop codon and truncate the Cx43 encoding sequence at the specified amino acid. This was performed using the InFusionHD™ cloning kit from Clontech, Inc. Primers are all listed in 5 to 3 prime order. Primers used for truncation/InFusion™ cloning used the same forward primer: Fwd-Cx43: CGGACTCAGATCTCGAGCTCAGATGGGTGACTGGAGTGCCTTG, and used alternate reverse primers: Bkwd-258t: AGAATTCGAAGCTTGAGCTCTTATGATGGGCTCAGTGGGCCAG, Bkwd-262t: AGAATTCGAAGCTTGAGCTCTTATCCGCAGTCTTTTGATGGGCTC, Bkwd-268t: AGAATTCGAAGCTTGAGCTCTTAGTAGGCGTATTTTGGAGATCCGCAG Bkwd-273t: AGAATTCGAAGCTTGAGCTCTTAGGAGCAGCCATTGAAGTAGGCGTAT.

Resulting PCR fragments containing truncated rat Cx43 coding sequence were inserted into the multiple cloning site 3-prime of the superfolderGFP sequence in the psfGFP-C1 plasmid linearized by the restriction digest enzyme SacI. sfGFP-Cx43C260Am268 was produced by InFusion cloning with a primer to mutate codon 260 in the Cx43 gene to alanine: Fwd-Vector: GACAATCGGCTGCTCTGATGCCGCC, Bkwd-Vector: CTTTTGATGGGCTCAGTGGGCCAGTGGTG, Fwd-Insert: TGAGCCCATCAAAAGACGCCGGATCTCC, Bkwd-Insert: GAGCAGCCGATTGTCTGTTGTGCCCAG.

The sfGFP-Cx43d20AA is rat Cx43 with twenty amino acids resected (residues 241-260). The un-tagged Cx43d20AA sequence was a kind gift from Drs. Steve Taffet and Mario Delmar (Homma, Alvarado et al. 1998). The Cx43 encoding sequence with the sectional deletion was copied by PCR and inserted into the sfGFP-C1 plasmid at the SacI recognition site, as described previously for full-length sfGFP-Cx43 and contains the same linker as all the other tagged sfGFP-Cx43 plasmids used in this study.

The sfGFP-Cx26CT43 plasmid contains the full-length rat Cx26 sequence with sequences encoding an amino-terminal sfGFP-tag linked in frame to the start of Cx26 by the same eight amino acid linker as the control sfGFP-Cx26 and with the sequence for rat Cx43 CT amino acid section from Cx43 residue K241 through S272 fused by a linker (ADPPVAT) between the terminal V226 of Cx26 and residue K241 of Cx43. Resulting plasmids were verified by sequencing.

Method of GJ plaque selection:

For 3D time-lapse FRAP experiments we searched the coverslip growth substrate for large fluorescent protein-tagged GJs oriented in a plane parallel with the growth substrate. For 2D time-lapse FRAP experiments we used each fluorescent protein plaque we identified that appeared to be, in our on-the-fly estimation, within +/- 15 degrees from perpendicular to the growth substrate and of at least 4.5 µm in length.

FRAP on heterotypic gap junction plaques:

FRAP experiments were performed on GJ plaques that formed between cells expressing cytoplasmic mCherry (mCherry as a co-expression marker in cells only co-transfected with untagged wildtype Cx43 or Cx43cyslCT) and cells without mCherry expression but having expression of either Cx43K258stop-msfGFP or Cx43-msfGFP. This produces functional GJ channels heterotypically tagged on one cell of the pair with msfGFP and the test connexin without a tag is in the membrane of the other cell. Since GJ docking/pairing is irreversible within live cells the tagged connexin acts as a location reporter for the untagged connexin. Since Cx43K258stop-msfGFP is highly mobile, heterotypic pairs of Cx43cyslCT::Cx43K258stop-msfGFP allowed us to test if un-tagged Cx43cyslessCT is mobile within GJ plaques.

FRAP analysis:

FRAP data analysis: FRAP analysis was performed as previously described (Stout, Snapp et al. 2015, Stout Jr and Spray 2016). Average fluorescence within the bleach region, for the entire GJ plaque to be bleached (Fluorescence pool available for recovery, Fp), and a portion of the background in a location with no GFP expression were outlined to generate 3 Regions Of Interest (ROI). Recovery curves were transformed to correct for loss of signal due to bleach and for acquisition-bleach of the total pool of fluorescent protein and normalized to 100% pre-bleach and 0% for the initial post-bleach time-point to normalize for incomplete bleaching within the bleach ROI as previously described (Snapp and Lajoie 2011). A correction factor (cf) was calculated by dividing the average of the 10 data points preceding the bleach for average fluorescence level of the fluorescent pool available for recovery (initial fluorescence pool; fpFo) by the fluorescent pool ROI readings at each time point after bleach (Fp), (fpFo/Fp). The bleach ROI reading (bF) for each time point was divided by the bleach region baseline-initial fluorescence Fo (bFo), (bF/bFo) and the resulting fraction of initial fluorescence was then multiplied by the correction factor. The resulting corrected fractional fluorescence was then multiplied by 100% to calculate the final “normalized, corrected and scaled recovery (%)” at each time-point.The normalized data points at 15 s after the bleach time-point were used in comparison of percent recovery at 15 s. Data for comparisons with two groups were analyzed by two-tailed Student’s T-test. Data for comparisons with more than two groups were analyzed by Analysis of Variance followed by Tukey’s multiple comparisons. Data was collected, scaled, and normalized in Microsoft Excel and then statistical comparisons were performed with Graphpad Prism 7 software.

Electrophysiology:

Isolated pairs of cultured N2A cells which do not normally display gap junction coupling that were plated onto four 12 cm glass coverslips inlayed into a 3.5 cm plastic cell culture dishes and then transfected using the same procedure as that used for FRAP experiments with DNA and transfection reagent-amount adjusted for the 3.5 cm culture dish (4 µg of DNA and 12 µL of Optifect reagent per 3.5 cm dish). 24-48 hours after transfection, isolated cell pairs expressing untagged Cx43cyslCT (rat Cx43C260,271,298A) were identified by cytoplasmic mCherry expression driven from a second promoter within the same plasmid as Cx43cyslCT and by lack of other adjacent cells by phase-contrast (Nikon Diaphot equipped for epifluorescence). For

electrophysiology cells were kept in external solution containing (in mM): NaCl 140, KCl 5, CsCl 2, $CaCl_2$ 2, $MgCl_2$ 1, HEPES 5, D-glucose 5, pyruvate 2, and $BaCl_2$ 1, pH 7.4, adjusted with NaOH. Patch pipette-electrodes were pulled with a P97 Flaming/Brown micropipette puller (Sutter Instrument Co.) and electrode resistances were 3-5 MΩ when filled with internal solution which contained (in mM): CsCl 130, EGTA 10, $CaCl_2$ 0.5, and HEPES 10, pH adjusted to 7.3 with CsOH. Dual whole cell voltage clamp was performed using Axopatch 1D amplifiers (Axon Instruments, Inc.) at room temperature (del Corsso, Srinivas et al. 2006). Data were acquired using pClamp10 software (Axon Instruments, Inc.). Cells were initially held at 0mV, given a brief 10 mV step pulse, then a voltage ramp was applied to one cell and the junctional current was recorded in the neighboring cell. Repeated sweeps of this protocol were performed in the presence of the GJ blocker heptanol (2mM) and junctional current was reduced leading to progressively smaller current ramps in both cells indicating GJ channel blockade.

Supplemental Figure Legends:

Supplemental Fig.1 Connexin mutants and fluorescent protein tagging strategy. **A)** The Cx43 protein sequence used in this study is shown, separated by a line near the point in the protein where the fourth and last transmembrane sequence transitions to the cytoplasmic carboxyl-terminus (the beginning of the CT). The location of the cysteine residues that stabilize the gap junction plaque are shown in red. Locations where the Cx43 CT is truncated for various mutants in Figure 1 of the main text are indicated. The highlighted section of the Cx43 sequence indicates the section that is resected to generate the sfGFP-Cx43d20AA sectional deletion mutant (Figure S4F). At right cartoons show the various truncation mutants with different amounts of truncation. The stabilizing cysteine residues are shown as red dots to indicate their presence or lack thereof in the case of the sfGFP-Cx43t258 truncation. Cartoons of cysteine to alanine mutants (Main text Figure 2, sfGFP-Cx43C260A,t268, and sfGFP-Cx43cyslCT) are shown with white filled circles indicating replacement of the stabilizing cysteines (shown in red) with alanine residues (white filled circles). The constructs illustrated are tagged with sfGFP on the amino terminus with a short linker between the sequence for the sfGFP and the first methionine in the connexin as described previously and in the main text. Untagged versions of Cx43 and Cx43cyslCT are the full-length wild-type and triple cysteine to alanine versions of rat Cx43 with no fluorescent protein fusion or linker. Those plasmids used for expression of untagged Cx43 contained mCherry driven by a separate promoter to identify transiently transfected cells and to indicate those cells that were not transfected with fluorescent protein-tagged connexin (see Supplemental Figure S2). **B)** The human Cx32 protein sequences used with the start of the CT marked and the two stabilizing cysteine residues shown in red. Cartoons at right illustrate the sfGFP-Cx32 and sfGFP-Cx32cyslCT constructs used for Figure 3 in the main text. **C)** The sequence for rat Cx26 used in this study is shown. Only five to six amino acids extend into the cytoplasm in the case of the Cx26 CT and it is not marked. The normal sfGFP-Cx26 construct used previously and the sfGFP-Cx26CT43 chimera that has the full length Cx26 sequence with the Cx43 CT (residues 241-272 appended at the CT of Cx26) are shown in cartoons to the right. Both constructs are tagged with sfGFP on the amino terminus with a short linker between the sequence for the sfGFP and the first methionine in the connexin as shown in Figure 1D of the main text. **D)** The amino acid sequence for human Cx30 used in this study and a cartoon at the right illustrating the EBFP2-Cx30 used in Figure 3C of the main text to form heterotypic gap junction plaques (EBFP2-Cx30::sfGFP-Cx32WT and EBFP2-Cx30::sfGFP-Cx32cyslCT).

Supplemental Fig.2 Approach to created heterotypically tagged gap junctions to test untagged and functional Cx43cyslCT mobility. **A)** Illustrated schematic showing the method of producing easily recognizable heterotypically tagged gap junction plaques. Note that in these and previous studies Cx43t258-msfGFP forms highly fluid gap junction plaques when homotypically or heterotypically tagged with monomerized superfolder GFP. The mCherry expression is driven from a different promoter (CMV) but is in the same plasmid as the untagged Cx43cyslCT and untagged Cx43full-length open reading frames to allow identification of cells transfected with untagged connexin constructs (driven from an EF1α promoter). **B)** Single plane confocal images of Neuro2A (N2A) cells showing the appearance of heterotypically tagged cells that are produced according to the scheme in "A". In the top panel the red and green channels are scaled to show the outline of the cells. Cx43t258-msfGFP connexons that have not yet docked and clustered into the gap junction (the GJ is the oversaturated green area indicated by the white triangle) demarcate the plasma membrane of the cell on the left (which only received transfection with CMV-Cx43t258-msfGFP). The blue arrows indicate sections of heterotypic plaque that have been endocytosed (endocytosis of gap junctions leads to internalization of connexin from the other cell). The second panel down in "B" is scaled to allow the morphology of the gap junction plaque to be visible (not oversaturated as in the panel above). The upper panels in "B" show the individual color channels scaled to make dim objects such as nonjunctional Cx43t258-msfGFP in the membrane and green intracellular vesicles in the red cell (produced during intercellular transfer of protein during gap junction endocytosis) visible. The larger amount of intracellular Cx43t258-msfGFP in the cell on the left is likely a combination of internalized gap junction vesicles, out-bound vesicles containing connexons/hemichannels, and ER/Golgi localized Cx43t258-msfGFP. **C)** Images of cells prepared as in the schematic above (Panel A). Three N2A cells imaged by a two channel, single focal plane confocal microscope acquisition. The cell in the center expresses only Cx43cyslCT + mCherry (red) while the cells on the left and right express Cx43t258-msfGFP. A fourth cell is almost entirely out of the field of view to the left edge of the image and it is also expressing Cx43t258-msfGFP. In this image a homotypically tagged Cx43t258-msfGFP::Cx43t258-msfGFP gap junction (both sides of the channels are the same) is on the left and in the same image a heterotypically tagged Cx43cyslCT::Cx43t258-msfGFP gap junction has formed on the right between the red cell and the rightmost cell (the untagged Cx43cyslCT in the red cells is not visible due to no fluorescent protein tag). Fluorescence was measured in a line scan perpendicular to the two gap junctions and the raw fluorescence of the heterotypically tagged gap junction is about half that of the homotypically tagged plaque joining the two cells to the left in the image. Line scan measurements were performed using ImageJ software on the first frame of a single channel (green) time-lapse FRAP experiment on the same cells in approximately the same location in the gap junction plaques as indicated with the small white boxes in the two-channel image shown in this figure and recorded from the time-point immediately prior to the FRAP experiment that was conducted on these cells (FRAP experiment not shown).

Supplemental Fig.3 Cx43 gap junction stability is not affected by intensity or duration of bleaching in HeLa cells. **A)** Other FRAP experiments in this study used 100% laser power, a scan speed of 5 and 3 iterations. The FRAP experiment in "A" was conducted on msfGFP-Cx43 using 10% laser power, a scan speed of 5, and 1 iteration. The top row shows raw images (cropped) from the 2D time-lapse FRAP experiment. Note the maintenance of sharp bleach borders (arrows) 1 minute and 50 seconds after the photobleaching event, although the bleaching was so light it is difficult to notice in the raw images. The second row in "A" shows the same images from the row above but scaled (Arbitrary Intensity Units, A.U., 1200-20000) to reveal the bleach region. Note the lack of recovery in the panel to the right indicated by the maintenance of the borders of the bleach region (indicated by white arrows). **B)** No recovery was observed with an intermediate level of bleach (same scan speed and 3 iterations with laser power reduced by 50%). **C)** Background subtracted unscaled, un-normalized traces from the two FRAP experiments shown above and traces generated on other cells using additional bleaching settings. Note the lack of substantial recovery of unbleached protein into the bleached region even with a very small percentage-bleach within the bleach region (green traces). The different bleach-laser power settings for each individual FRAP experiment is listed at right. Recovery was not observed even with the "gentlest" bleaching settings. Differences in brightness of the msfGFP-Cx43 gap junction plaques and background are likely due to imperfections in coverglass (growth substrate) thickness and/or differing distances between the gap junction plaque and the growth substrate. Orientation of the gap junction plaque also has an effect on apparent brightness in confocal imaging.

Supplemental Fig.4 Cysteines control GJ plaque arrangement stability in mouse Neuro2A cells and additional supporting evidence from HeLa cells. **A)** Cysteine residues stabilize sfGFP-Cx43 GJ plaques- sfGFP-Cx43cyslCT recovery is significantly higher at 15 s post-bleach in 2D time-lapse FRAP in Neuro2A (N2A) cells. **B)** Cysteine residues in the carboxyl-terminus of untagged and channel-functional Cx43 GJ plaques stabilize GJ plaque arrangement at 15 s in N2A cells. **C)** Cysteine residues in the Cx32 carboxy-terminus stabilize the GJ plaque in N2A cells. **D)** The significant effect of 10 mM DTT treatment was not found in N2A cells expressing sfGFP-Cx43, although a trend toward increased fluidity was observed with the reducing agent. **E)** DTT treatment (10 mM, 6 hr) did not significantly affect plaque stability for GJs composed of the already fluidly arranged sfGFP-Cx43cyslCT in N2A cells. **F)** In HeLa cells, percent recovery at 15 s post-bleach for sfGFP-Cx43 with a sectional deletion of 20 amino acids (sfGFPCx43d20AA, with K241-C260 resected). Recovery at 15 s for sfGFP-Cx43d20AA is compared to relevant groups with data sourced from other parts of this figure, and showing that sfGFP-Cx43d20AA arrangement within the plaque is similar to full-length sfGFP-Cx43. A portion of the original image data for msfGFP-Cx43, and sfGFP-Cx43t258 was sourced from the data used for the Stout et. al. 2015 *JBC* study and re-analyzed with additional new data for those groups. **G)** Pilot experiments with a variety of pharmacological agents did not have a noticeable effect on GJ plaque stability. Data are presented as percent recovery at 15 s post-bleach as elsewhere in this report in interest of simplicity, but it is clearly evident when an agent has no effect on GJ plaque stability and further experiments were not conducted. No effect on gap junction plaque stability was noted for inhibitors of palmitoylation (2-Bromohexadecanoic acid,

50 µM >12 hours), nitric oxide synthase inhibitor Nω-nitro-L-arginine (L-NNA, 100 µM 8 hours), Sulfhydration (H2S donor, NaHS, 50 µM 1 hour), or Zn^{2+} and Cu^{2+}chelator N,N,N',N'-tetrakis(2-pyridylmethyl)ethylenediamine (TPEN, 60µM 3 hours) in cells expressing normally stable gap junctions. Results from experiments from HeLa cells and experiments from N2A cells expressing sfGFP-Cx43 and sfGFP-Cx43t262 are combined since no difference was observed between these normally stable constructs or with regard to cell type. **H-K)** X-Y scatter plots of the percent recovery at 15 s (Y) and GJ plaque length in two dimensions as measured in the 2D time-lapse FRAP experimental image data from HeLa cells that was used for the main figures of this report.

Supplemental Video:

The included video has 3 Parts. Part 1) Shows a computer generated animation to orient the viewer to the spatial arrangement of the experimental data shown in Parts 2 and 3. CGI rendering produced in Blender v2.77 (blender.org) Part 2) Shows a real experimental FRAP experiment (3D reconstructions at each time point from 11 confocal planes) on a GJ plaque in N2A cells transfected with sfGFP-Cx43 (wild-type, cysteines are present). Note that there is essentially no recovery of unbleached sfGFP-Cx43 into the bleach region. Part 3) Shows a 3D-timelapse FRAP experiment in N2A cells transfected with sfGFP-Cx43cyslCT. Note the rapid diffusion of unbleached sfGFP-Cx43 into the bleach region. Also note that the perimeter of the plaque is less fluid for the stably arranged plaque (Cx43 WT, Part 2) than the fluid plaque (Cx43cyslCT, Part 3) indicating that there are substantial differences in stability in the WT and cysteine mutant forms of Cx43 in plaque regions remote from the bleach location and that the effect of the stabilizing cysteine residues we report are not an artifact of photobleaching. Video assembled and captioned in Adobe Premiere Pro CC™.

SUPPLEMENTAL REFERENCES

Stout, R. F., Jr., E. L. Snapp and D. C. Spray (2015). "Connexin Type and Fluorescent Protein Fusion Tag Determine Structural Stability of Gap Junction Plaques." J Biol Chem **290**(39): 23497-23514.

Homma, N., J. L. Alvarado, W. Coombs, K. Stergiopoulos, S. M. Taffet, A. F. Lau and M. Delmar (1998). "A particle-receptor model for the insulin-induced closure of connexin43 channels." Circ Res **83**(1): 27-32.

Stout, R. F., Jr., E. L. Snapp and D. C. Spray (2015). "Connexin Type and Fluorescent Protein Fusion Tag Determine Structural Stability of Gap Junction Plaques." J Biol Chem **290**(39): 23497-23514.

del Corsso, C., M. Srinivas, M. Urban-Maldonado, A. P. Moreno, A. G. Fort, G. I. Fishman and D. C. Spray (2006). "Transfection of mammalian cells with connexins and measurement of voltage sensitivity of their gap junctions." Nat Protoc **1**(4): 1799-1809.
Homma, N., J. L. Alvarado, W. Coombs, K. Stergiopoulos, S. M. Taffet, A. F. Lau and M. Delmar (1998). "A particle-receptor model for the insulin-induced closure of connexin43 channels." Circ Res **83**(1): 27-32.
Snapp, E. L. and P. Lajoie (2011). "Photobleaching regions of living cells to monitor membrane traffic." Cold Spring Harb Protoc **2011**(11): 1366-1367.
Stout Jr, R. F. and D. C. Spray (2016). FRAP for the Study of Gap Junction Nexus Macromolecular Organization. Gap Junction Channels and Hemichannels, CRC Press**:** 63-91.
Stout, R. F., Jr., E. L. Snapp and D. C. Spray (2015). "Connexin Type and Fluorescent Protein Fusion Tag Determine Structural Stability of Gap Junction Plaques." J Biol Chem **290**(39): 23497-23514.

Stout et. al. Figure S1. Connexin protein sequences and tagging strategies used in this study

A. Rat Cx43 sequence and tagging-schemes **(Fig.1,2,4)**

MGDWSALGKLLDKVQAYSTAGGKVWLSVLFIFRILLLGTAVESAWGDEQS
AFRCNTQQPGCENVCYDKSFPISHVRFWVLQIIFVSVPTLLYLAHVFYVM
RKEEKLNKKEEELKVAQTDGVNVEMHLKQIEIKKFKYGIEEHGKVKMRGG
LLRTYIISILFKSVFEVAFLLIQWYIYGFSLSAVYTCKRDPCPHQVDCFL
SRPTEKTIFIIFMLVVSLVSLALNIIELFYVFFKGVKDRVKGRSDPYHAT
TGPLSPSKD C GSPKYAYFNGCSSPTAPLSPMSPPGYKLVTGDRNNSSCRN
YNKQASEQNWANYSAEQNRMGQAGSTISNSHAQPFDFPDDNQNAKKVAAG
HELQPLAIVDQRPSSRASSRASSRPRPDDLEI

Start of CT at ~K234

t258 t268 t273

Cysteine Anchoring Domain (AD)

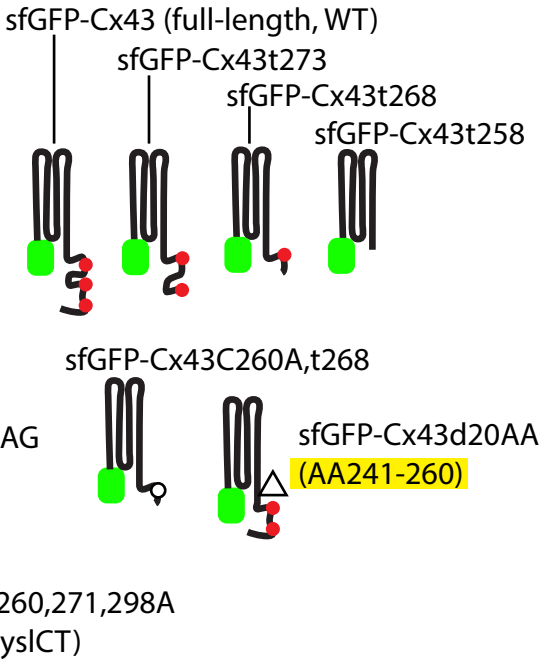

B. Human Cx32 sequence and tagging-schemes **(Fig. 3,4)**

MNWTGLYTLLSGVNRHSTAIGRVWLSVIFIFRIMVLVVAAESVWGDEKSS
FICNTLQPGCNSVCYDQFFPISHVRLWSLQLILVSTPALLVAMHVAHQQH
IEKKMLRLEGHGDPLHLEEVKRHKVHISGTLWWTYVISVVFRLLFEAVFM
YVFYLLYPGYAMVRLVKCDVYPCPNTVDCFVSRPTEKTVFTVFMLAASGI
CIILNVAEVVYLIIRACARRAQRRSNPPSRKGSGFGHRLSPEYKQNEINK
LLSEQDGSLKDILRRSPGTGAGLAEKSDRCSACStart of CT

C. Rat Cx26 sequence and tagging-schemes **(Fig. 1)**

MDWGTLQSILGGVNKHSTSIGKIWLTVLFIFRIMILVVAAKEVWGDEQAD
FVCNTLQPGCKNVCYDHYFPISHIRLWALQLIMVSTPALLVAMHVAYRRH
EKKRKFMKGEIKNEFKDIEEIKTQKVRIEGSLWWTYTTSIFFRVIFEAVF
MYVFYIMYNGFFMQRLVKCNAWPCPNTVDCFISRPTEKTVFTVFMISVSG
ICILLNITELCYLFIRYCSGKSKRPV

Appended Sequence in GFP-Cx26CT43A

Linker Cx43 CT AA241-272

ADPPVAT KGRSDPYHATTGPLSPSK

DCGSPKYAYFNGCS

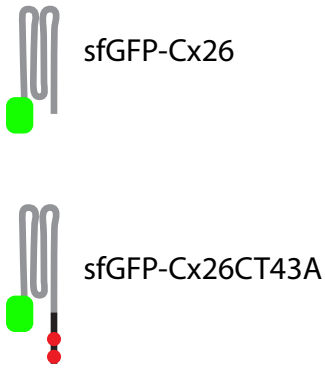

D. Human Cx30 sequence and tagging-schemes **(Fig. 3)**

MDWGTLHTFIGGVNKHSTSIGKVWITVIFIFRVMILVVAAQEVWGDEQED
FVCNTLQPGCKNVCYDHFFPVSHIRLWALQLIFVSTPALLVAMHVAYYRH
ETTRKFRRGEKRNDFKDIEDIKKQKVRIEGSLWWTYTSSIFFRIIFEAAF
MYVFYFLYNGYHLPWVLKCGIDPCPNLVDCFISRPTEKTVFTIFMISASV
ICMLLNVAELCYLLLKVCFRRSKRAQTQKNHPNHALKESKQNEMNELISD
SGQNAITGFPSStart of CT

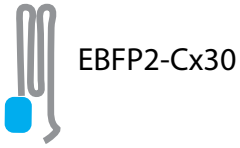

Stout et. al. Figure S3. Varied bleach strength

A. msfGFP-Cx43 FRAP bleached with 10% laser power, scan speed 5, 1 bleach iteration

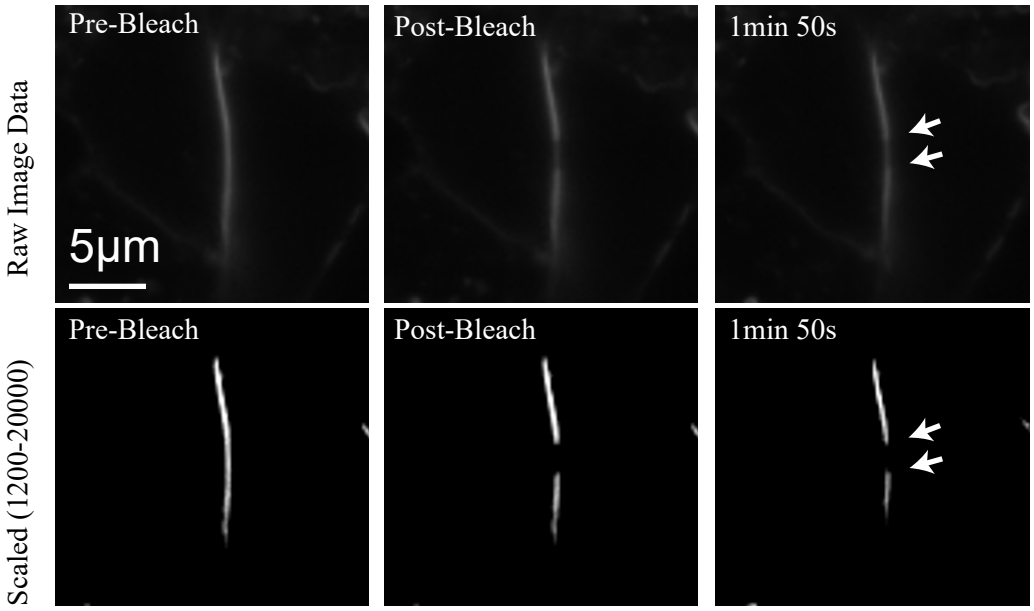

B. msfGFP-Cx43 FRAP bleached with 50% laser power, scan speed 5, 3 bleach iterations

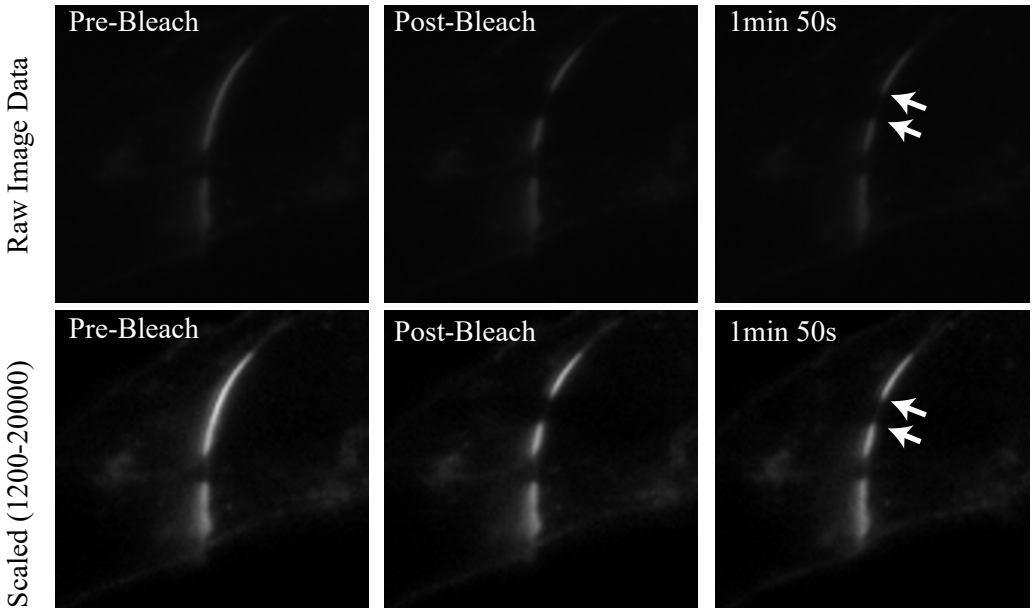

C. msfGFP-Cx43 FRAP with Varied Bleaching Power and Time

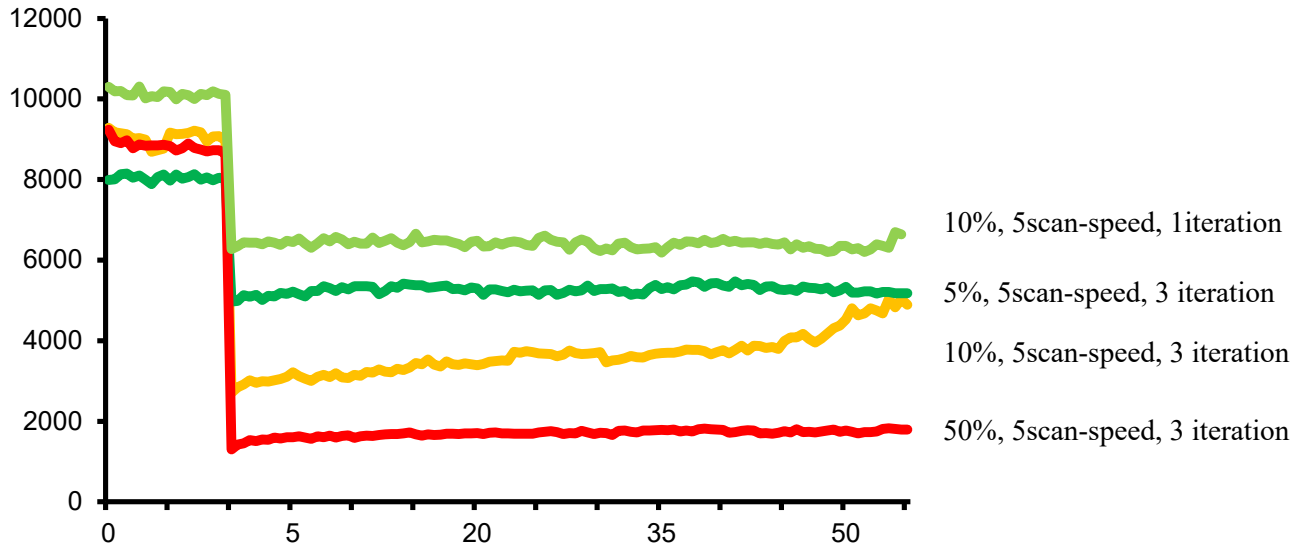

Stout et. al. Figure S2. FRAP to measure mobility of untagged connexins

A. Culture-scheme for FRAP on untagged Cx43

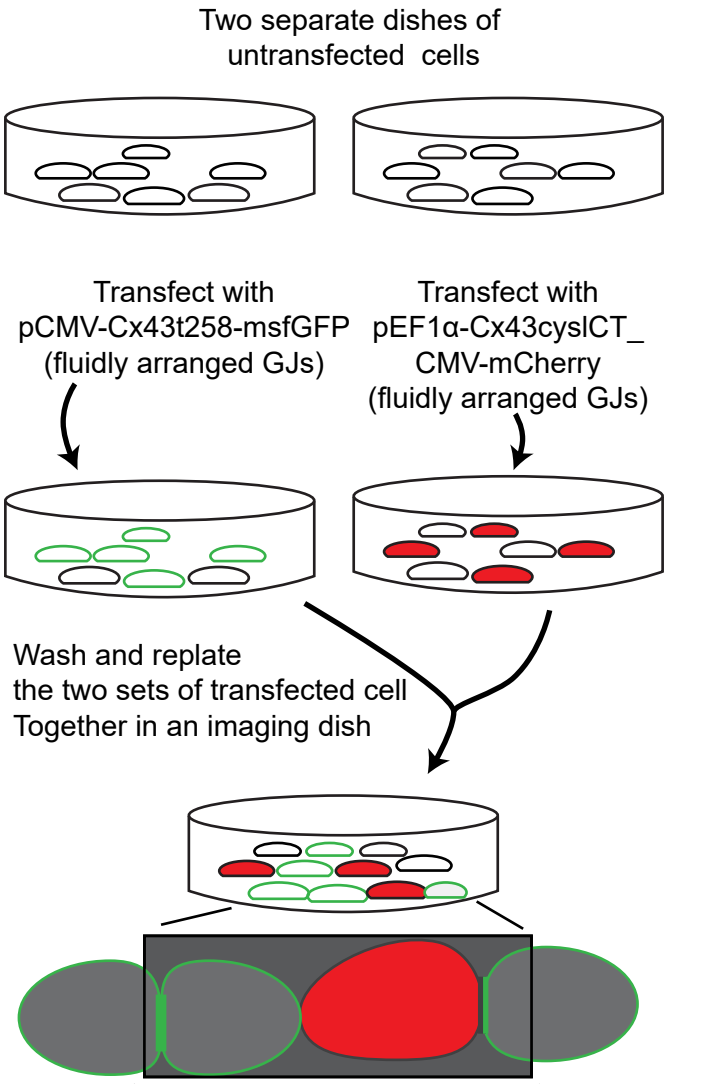

B. Single plane confocal image of a pair of cells with a heterotypically tagged gap junction

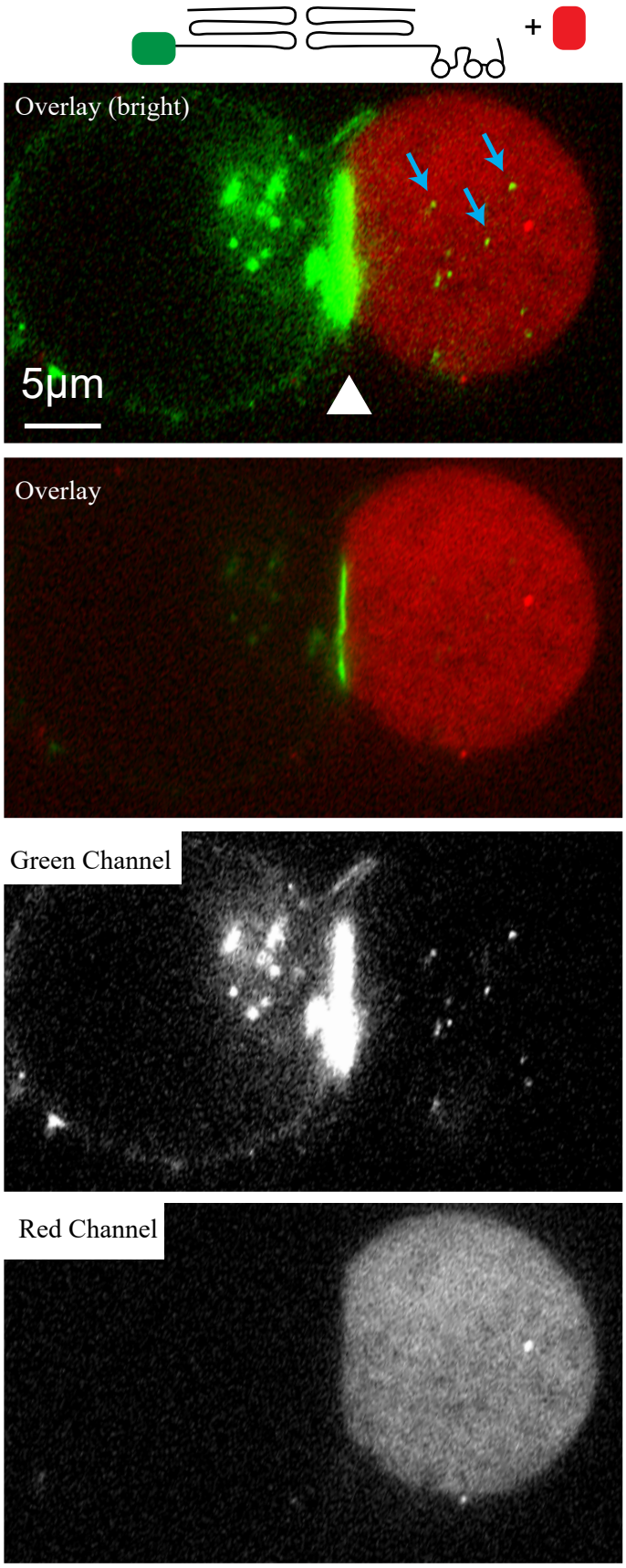

C. Line-scans show halved GJ plaque brightness

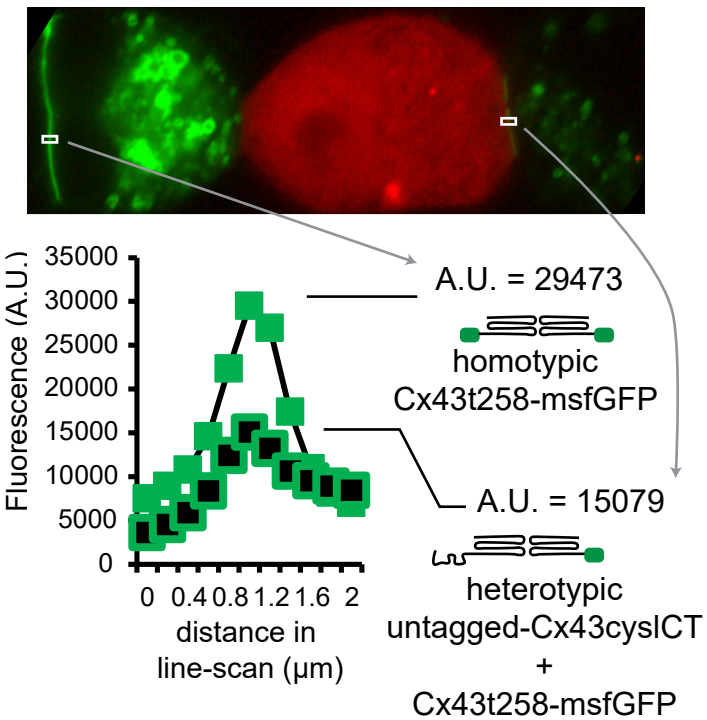

Stout et. al. Figure S4. Other cell types, mutants, and fluorescent protein tags

Stout et. al. Figure S5.